Physics – Uspekhi **61** (7) 698 – 706 (2018)

CONFERENCES AND SYMPOSIA PACS numbers: **75.78. – n**, **77.84. – s**

Dielectric resonant magnetic dipoles: paradoxes, prospects, and first experiments

A B Shvartsburg, V Ya Pecherkin, L M Vasilyak, S P Vetchinin, V E Fortov

DOI: https://doi.org/10.3367/UFNe.2017.03.038139

Contents

Abstract. **We review various forms of dielectric ring-shaped oscillating circuits excited by displacement currents due to the grazing incidence of GHz microwaves. Such circuits with azimuth displacement currents form resonant dielectric magnetic dipoles. We calculate and measure resonances in field spectra in the near zone of such dipoles. We demonstrate the inversion of the magnetic inductance flux and the formation of a negative magnetic permeability in the resonant range of dielectric magnetic dipoles. We also investigate, both analytically and experimentally, the resonant interaction spectra of a pair of magnetic dipoles excited by displacement currents. Finally, prospects for using these dipoles to model all-dielectric nanostructures with alternating-sign magnetic permeability are discussed.**

Keywords: displacement current, dielectric metamaterial, dielectric magnetic dipole, interaction of resonant dipoles, negative magnetic permeability

1. Introduction

This paper is concerned with the effect of resonance electromagnetic induction in a nonconducting dielectric medium. Variation in the magnetic field in such media excites displacement currents, which, in contrast to conduction currents, are proportional not to the electric field but to the rate of its variation. Specifically, we discuss displacement currents and microwave (MW) fields in all-dielectric subwavelength structures devoid of free carriers and the possible transfer of these effects to the optical region. The last 10–15 years have witnessed a rapid growth of interest in these phenomena, and investigations are stimulated by several problems, both applied and academic.

(1) A trend has arisen to replace metallic radio electronic elements with subwavelength low-loss dielectric structures of artificial materials — metamaterials. Fabricating these materials opens up the possibility to optimally combine electric and magnetic parameters, including unusual effects like controllable nonlocal dispersion [1], nonzero or negative permittivity [2], and negative magnetic susceptibility [3].

(2) The exchange of concepts between radio engineering and laser optics has led to the formation of a separate area of wave physics, radio optics [4]. Following this trend, several key components of MW electronics with capacitance and inductance properties have been developed in the optoelectronics of nanodimensional metamaterials in recent years. This new area has received a special name: metatronics [5]. The generalization of electromagnetic induction effects, which are traditionally associated with conduction currents in metals, to the case of displacement currents in dielectrics shows specific ways to minimize losses and miniaturize optoelectronic systems: for a high permittivity and low dielectric loss, the dimensions of dielectric resonators are substantially smaller than those of metallic ones.

(3) A radically new problem has arisen: controlling the magnetic components of the light field in the optical and infrared (IR) ranges with the use of dielectric magnetic structures: so-called optical magnetism [6]. The dielectric magnets under consideration have nothing in common with either the magnetic dielectrics [7] or the magnetooptics [8], despite the likeness of the names: the task involves the development of nanodimensional oscillatory systems and

A B Shvartsburg Joint Institute for High Temperatures,
Russian Academy of Sciences,
ul. Izhorskaya 13, str. 2, 125412 Moscow, Russian Federation;
Space Research Institute, Russian Academy of Sciences,
ul. Profsoyuznaya 84/32, 117997 Moscow, Russian Federation;
Far Eastern Federal University,
ul. Sukhanova 8, 690950 Vladivostok, Russian Federation
E-mail: alex-s-49@yandex.ru
V Ya Pecherkin, L M Vasilyak, S P Vetchinin, V E Fortov
Joint Institute for High Temperatures,
Russian Academy of Sciences,
ul. Izhorskaya 13, str. 2, 125412 Moscow, Russian Federation

Received 5 April 2017
Uspekhi Fizicheskikh Nauk **188** (7) 780 – 789 (2018)
DOI: https://doi.org/10.3367/UFNr.2017.03.038139
Translated by E N Ragozin; edited by A M Semikhatov

the generation of magnetic modes already proven in the GHz range [9].

In this paper, we discuss the first group of results related to the development of a new class of all-dielectric oscillatory systems operating by displacement currents. Some characteristic features of such currents and the generation of magnetic modes in the resonance scattering of electromagnetic waves by dielectric bodies (Mie scattering) are discussed in Sections 2 and 3. Another resonance excitation mechanism, which leads to the formation of a resonance dielectric magnetic ring dipole and negative magnetic induction, is considered in Sections 4 and 5. The near-field resonance interaction spectra of such dipoles are presented in Section 6. Discussed in the concluding Section 7 are the possibilities of using resonant magnetic dipoles for modeling dielectric nanooptical structures.

2. Electrodynamics of displacement currents

The concept of the displacement current and the name itself were introduced by Maxwell nearly 150 years ago when explaining the operation of the Thomson oscillating circuit. Early in his scientific career, W Thomson, one of the founding fathers of the first transatlantic telegraph and the originator of the absolute temperature scale, who was conferred the title of Baron Kelvin in recognition of his achievements, made the first device for generating electric current oscillations. The device was an electric circuit comprising a battery, a capacitor, and an inductance coil. In the course of the capacitor discharge, the electric current passed through the coil to excite a magnetic field, and then the decay of the magnetic field excited the current, which recharged the capacitor. The energy of the system periodically transferred from the capacitor to the coil and back. This 'electric pendulum' entered textbooks as the 'Thomson oscillating circuit'.

However, this novelty immediately revealed a paradox: unlike the currents flowing through conductors, the alternating current penetrated through the empty gap between the capacitor plates, and hence there was a break in the flow of current. On the other hand, the current continuity, understood by analogy with the continuity of liquid flow in a tube seemed quite evident. Several years later, the conflict between theory and experiment was resolved by Maxwell, who surmised that a variation in the electric induction **D** in time excited a magnetic field **H**. Calling the usual current in a conductor the 'conduction current', Maxwell endowed his innovation with the name 'magnetic displacement current' and gave the formula for calculating the density of this current:

$$\mathbf{j} = \frac{1}{4\pi}\frac{\partial \mathbf{D}}{\partial t}\,. \tag{1}$$

In the framework of the theory of ether accepted at the time, the new term related the variation in the electric induction to the displacement of ether particles. The new notion enabled Maxwell, in his *A Treatise on Electricity and Magnetism* (1873), to write the fundamental system of electrodynamic equations and predict the existence of a special kind of oscillations — electromagnetic waves.

The notions of displacement currents and electromagnetic waves did not immediately take root in the physical community, and Maxwell himself did not live to witness the triumph of his equations. We recall that at the end of the 19th century, electric motors, lighting, and incipient telephony harnessed usual conduction currents in metals, while the nonconductive dielectrics were assigned the part of insulators. By contrast, the 'displacement current' seemed to be a mathematical phantom inserted into one of Maxwell's equations to maintain the continuity of alternating current lines in a nonconductive medium. Actually, this new object of electrodynamics, although termed 'current', had little in common with the established laws of conduction currents, which were the physical foundation of electrical engineering. Unlike the conduction current, the displacement current was not described by Ohm's law, was not localized in wires, and was unusable for electric heating. Several years after the publication of Maxwell's *Treatise*, Heinrich Hertz, when experimenting on sparks in gaps, clearly demonstrated the propagation of electromagnetic waves through empty space separating the gaps. Furthermore, in another experiment, these waves passed through a dielectric layer (a concrete plate). After the discovery of electromagnetic wave propagation in nonconductive media, the adjective 'magnetic' fell away from the definition of the displacement current and the concept itself was universally recognized.

3. Resonance scattering from dielectric bodies (Mie resonances)

The last decade has been marked by a rapid development of a new area in the electrodynamics of continuum media aimed at the design of dielectrics with the desired spectral and spatial characteristics of magnetic response in the GHz, THz, and IR ranges. Apart from the magnetization problem of uniform semiconductors with free electrons in the field of an electromagnetic wave [10], discussion is underway regarding ways of developing inhomogeneous metamaterials whose magnetic properties are provided by nanodimensional dielectric inclusions of the requisite shape [11, 12]. These inclusions act as resonators with their own eigenmodes. The spectra of such modes are defined by Mie resonances.

A simple example of the formation of a Mie resonance is provided by the problem of the scattering of a plane wave by an infinite uniform dielectric cylinder [13]. We consider the propagation of a linearly polarized wave along the z axis. The magnetic components of the incident and scattered fields and of the field inside the cylinder, H_z^{inc}, H_z^{sc}, and H_z^{int}, are solutions of the wave equation in the form of Bessel functions J_m and zeroth-order Hankel functions $H_m^{(1)}$:

$$\begin{aligned} H_z^{\mathrm{inc}}(kr) &= H_0 \sum_m \mathrm{i}^m J_m(kr)\exp(\mathrm{i}m\phi)\,,\\ H_z^{\mathrm{sc}}(kr) &= -H_0 \sum_m \mathrm{i}^m a_m H_m^{(1)}(kr)\exp(\mathrm{i}m\phi)\,,\\ H_z^{\mathrm{int}}(nkr) &= H_0 \sum_m \mathrm{i}^m c_m J_m(nkr)\exp(\mathrm{i}m\phi)\,. \end{aligned} \tag{2}$$

The coefficients a_m and c_m in Eqns (2) are determined from the boundary conditions of the wave field continuity on the cylinder surface:

$$a_m = \frac{1}{\Delta}\left[J_m(\xi)\,\frac{\mathrm{d}J_m(n\xi)}{\mathrm{d}\xi} - n\,J_m(n\xi)\,\frac{\mathrm{d}J_m(\xi)}{\mathrm{d}\xi}\right], \tag{3}$$

$$c_m = \frac{J_m(\xi) - a_m H_m^{(1)}(\xi)}{J_m(n\xi)}\,, \tag{4}$$

$$\Delta = H_m^{(1)}(\xi)\,\frac{\mathrm{d}J_m(n\xi)}{\mathrm{d}\xi} - n\,J_m(n\xi)\,\frac{\mathrm{d}H_m^{(1)}(\xi)}{\mathrm{d}\xi}\,, \qquad (5)$$

$$\xi = \frac{2\pi a}{\lambda}\,, \qquad m = 0, 1, 2, \ldots\,.$$

In expressions (2)–(5), n and a are the refractive index and the cylinder radius, and λ is the wavelength of the incident wave.

Magnetic effects in this structure are due to displacement currents $\mathbf{j}_\mathrm{d}$. These currents, which are caused by the alternating electric induction $\mathbf{D}$ (1) inside the cylinder in the planes perpendicular to the cylinder axis, can increase many-fold when the geometric parameter ξ in Eqn (5) corresponds to one of the eigenmodes of field oscillations inside the cylinder. By equating the denominator in expression (3) for a_m to zero, we obtain an equation for the Mie resonances of order m in the scattering from the cylinder: $\Delta = 0$. Under such a resonance, the values of the coefficient c_m in (4) increase as Δ^{-1} and the field inside the cylinder is defined by the function $J_m(nkr)$. This resonance can enhance the magnetic effects of nonmagnetic dielectric inclusions. Such an increase in the magnetic field inside a long hollow cylinder filled with distilled water at a temperature of 363 K with a relative permittivity of 58 was observed in [14]. However, the magnetic flux does not concentrate entirely inside the cylinder and, decaying outside the cylinder, makes a kind of 'halo' around it [15].

A similar consideration of the scattering of a linearly polarized wave on a ball permits finding the eigenmode spectrum of a uniform dielectric ball. The resonance frequency of the mth mode is defined by the equation [16]

$$J_m(\theta\xi)\,\frac{\mathrm{d}H_m^{(1)}(\xi)}{\mathrm{d}\xi} - \theta^{2p-3}H_m^{(1)}(\xi)\,\frac{\mathrm{d}J_m(\theta\xi)}{\mathrm{d}\xi} = 0\,, \qquad (6)$$

where J_m and $H_m^{(1)}$ are the spherical Bessel and Hankel functions, the value of p corresponds to the TM polarization ($p = 1$) or the TE polarization ($p = 2$) of the wave, ξ is a geometric parameter, and θ is the relative refractive index:

$$\xi = \frac{2\pi a n_\mathrm{med}}{\lambda}\,, \qquad \theta = \frac{n_p}{n_\mathrm{med}}\,, \qquad (7)$$

where n_p and n_med are the refractive indices of the ball material and the environment. The eigenmodes for silicon nanospheres embedded in a silver matrix are described in Ref. [17]. For a nonuniform sphere with a radially symmetric step-wise profile of the refractive index, the resonance frequencies were found in Ref. [18].

The exact analytic solutions of the wave equation for the scatterer eigenmode spectra are known for an infinitely long cylinder [13] and a sphere [19]. The resonance regimes of Mie scattering by a disk and a cone were investigated numerically in Ref. [20]. More general numerical techniques for the analysis of magnetic modes in nonspherical axially symmetric bodies, which are based on an approximate solution of integral equations, were developed in Ref. [21]. It is noteworthy that some bodies of rotation, for instance open dielectric resonators operating at gigahertz frequencies, have long been used in microwave engineering. Specifically, given a solution of the Maxwell equations in the diffraction approximation, it was possible to determine the symmetric types of the eigenmodes of different dielectric ring resonators in relation to their dimensions and the permittivity ε. In particular, the number of lowest-mode radial eigen-oscillations for dielectric rings with high ε values was shown to be much smaller than for continuous dielectric cylindrical resonators. In this case, the numerical solution of the boundary value problem for the eigenfrequencies of a dielectric ring resonator obtained for several sets of geometric parameters is limited to the domain of positive magnetic response. Solving the electrodynamic problem exactly is hindered by the presence of open boundary surfaces with abrupt changes in ε at the interfaces between the media and the necessity of including diffraction effects in the scattering of waves at such interfaces. No solutions were obtained for a thin dielectric ring, in which only azimuthal oscillations are induced [22].

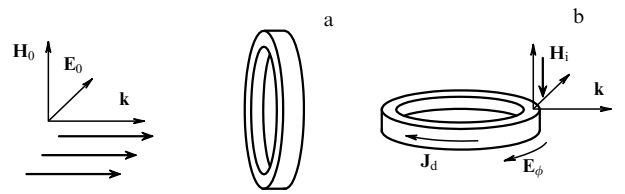

Figure 1. Scattering geometry of a linearly polarized plane wave with components $\mathbf{E}_0$ and $\mathbf{H}_0$ and wave vector $\mathbf{k}$. (a) Normal incidence, the ring's plane is perpendicular to vector $\mathbf{k}$. (b) Grazing incidence, the ring's plane is perpendicular to the magnetic component of the incident wave $\mathbf{H}_\mathrm{i}$. The arrangement shown in Fig. 1b is used in experiments in the resonance excitation of displacement current oscillations in the dielectric ring circuit. $\mathbf{J}_\mathrm{d}$ and $\mathbf{E}_\phi$ are the azimuthal displacement current and the vortical electric field induced in the circuit.

Below, we consider the resonance response in the case of grazing incidence of a plane wave on a thin dielectric ring, which corresponds to the geometry shown in Fig. 1b. In this case, the fundamental azimuthal mode of field oscillations and the azimuthal displacement current are excited in the ring circuit. The circuit around which the displacement current flows makes up a peculiar dielectric magnetic dipole. The spectra of the fields of this dipole are distinguished by several features:

(a) the dominant effect of the small radius of the ring on its resonance properties;

(b) the inversion of magnetic induction and the emergence of negative magnetic susceptibility of the ring circuit;

(c) the resonance interaction of a pair of magnetic dipoles.

In what follows, we discuss theoretical and experimental investigations of these effects.

4. Dielectric magnetic dipole and the Thomson oscillating circuit

In Thomson's oscillating circuit, the capacitance and the inductance were formed by separate elements: a capacitor and an inductance coil. A similar 'separation of functions' was also used in Pendry's split-ring resonator [23], which consisted of two concentric metallic rings (inductor) with cuts (capacitor). In contrast, below, we discuss the oscillation modes of an uncut dielectric ring with $\varepsilon \gg 1$, which combines both indicated functions.

We consider the interaction of an electromagnetic wave with a thin dielectric ring of circular cross section, whose major and minor radii R and r_0 satisfy the condition $R \gg r_0$. A linearly polarized plane wave with a wave vector k is incident in the x direction, such that the magnetic component of the

wave field $H_0 \exp[\mathrm{i}(kx - \omega t)]$ is aligned with the z axis perpendicular to the ring plane xy. The electric field $\mathbf{E}$ of the wave is aligned with the y axis (Fig. 1b).

The magnetic flux of this component through the circular circuit is expressed as

$$\Phi_0 = H_0 F \exp(-\mathrm{i}\omega t)\,, \qquad F = \int \exp(\mathrm{i}kx)\,\mathrm{d}S\,. \tag{8}$$

The integral in expression (8) is taken over the area inside the ring of the radius R and is expressed in terms of the Bessel function J_1 [24]:

$$F = \pi R^2 f(kR) \exp\left[\mathrm{i}(kR - \omega t)\right], \quad f(kR) = \frac{2J_1(kR)}{kR}\,. \tag{9}$$

Induced in the ring is an azimuthal current I, which, in turn, generates a magnetic induction flux Φ_i, with the total induction flux through the ring given by $\Phi = \Phi_0 + \Phi_\mathrm{i}$. The vortical emf U and the electric field E_ϕ induced in the ring are defined by the variation in the flux Φ:

$$U = -\frac{1}{c}\frac{\partial \Phi}{\partial t}\,, \qquad E_\phi = \frac{U}{2\pi R}\,. \tag{10}$$

A further analysis of the magnetic effects of a ring circuit depends on the circuit conduction. These effects are convenient to illustrate by comparing the currents I induced by the same alternating magnetic fluxes Φ_0 in two similar thin rings, one of which is made of a conductor with a conductivity σ and the other of a dielectric with a permittivity ε (Fig. 1b). The temporal and spectral dependences of the current I are radically different in the cases of conductive and nonconductive circuits: the conduction current density j_c depends on the first derivative of the flux Φ, while the displacement current density j_d, which is induced in the nonconductive dielectric circuit, is determined by the second derivative of Φ:

$$j_\mathrm{c} = -\frac{\sigma}{2\pi Rc}\frac{\partial \Phi}{\partial t}\,, \qquad j_\mathrm{d} = -\frac{\varepsilon}{8\pi^2 Rc}\frac{\partial^2 \Phi}{\partial t^2}\,. \tag{11}$$

Considering the residual conductivity of the dielectric and using the expression for the self-induction L of a thin ring [8], the magnetic induction flux Φ_i in the ring plane can be represented as

$$\Phi_\mathrm{i} = \frac{LI}{c}\,, \qquad L = 4\pi R l\,, \qquad l = \ln\left(\frac{8R}{r_0}\right) - \frac{7}{4}\,, \qquad I = \pi r_0^2 (j_\mathrm{c} + j_\mathrm{d})\,. \tag{12}$$

We substitute relations (12) in the expression for the total magnetic induction flux $\Phi = \Phi_0 + \Phi_\mathrm{i}$ to obtain an equation for the flux Φ through the circuit:

$$\frac{\partial^2 \Phi}{\partial t^2} + \gamma\frac{\partial \Phi}{\partial t} + \omega_0^2 \Phi = \omega_0^2 \Phi_0\,. \tag{13}$$

The circuit eigenfrequency ω_0 and the damping decrement γ in Eqn (13) are defined by the formulas

$$\omega_0^2 = \frac{2c^2}{\varepsilon l r_0^2}\,, \qquad \gamma = \frac{4\pi\sigma}{\varepsilon}\,. \tag{14}$$

The solution of Eqn (13) can be represented in the form

$$\Phi = \Phi_0 \Lambda(\omega) \exp(-\mathrm{i}\omega t)\,, \qquad \Lambda(\omega) = \frac{\omega_0^2}{\omega_0^2 - \omega^2 - \mathrm{i}\omega\gamma}\,. \tag{15}$$

Expression (15) for the magnetic flux suggests that the dielectric ring with an azimuthal current (Fig. 1b) can be regarded as a resonance magnetic dipole excited by the displacement current, with the resonance effect near the frequency ω_0 described by the factor $\Lambda(\omega)$. The displacement current I_d calculated by substituting formula (15) in expression (11) also contains the resonance factor $\Lambda(\omega)$:

$$I_\mathrm{d} = \frac{\varepsilon r_0^2 \omega^2 \Lambda(\omega) \Phi_0 \exp(-\mathrm{i}\omega t)}{8\pi Rc}\,. \tag{16}$$

From the known current I_d, we can find the vector potential A_ϕ of this current and express the components of the electromagnetic field induced by the current I_d in the near-field zone of the ring in terms of A_ϕ:

$$A_\phi = \frac{2IR}{c}\aleph\,, \qquad \aleph = \int_0^\pi \mathrm{d}\phi\,\frac{\exp(\mathrm{i}kr)}{r}\cos\phi\,. \tag{17}$$

The variables r and ϕ in integral (17) are the distance from the ring center and the azimuthal angle in the ring plane. The vortical electric field E_curl and the magnetic field components H_z and H_ρ outside the ring are expressed in terms of A_ϕ as [8]

$$E_\mathrm{curl} = -\frac{1}{c}\frac{\partial A_\phi}{\partial t}\,, \quad H_z = \frac{\partial A_\phi}{\partial \rho} + \frac{A_\phi}{\rho}\,, \quad H_\rho = -\frac{\partial A_\phi}{\partial z}\,. \tag{18}$$

The near-field ($kr \ll 1$) spectrum of E_curl calculated from expressions (16)–(18) is conveniently expressed in dimensionless form as

$$\frac{E_\mathrm{curl}}{H_0} = \frac{\mathrm{i}R^2\omega^3\Lambda(\omega)\aleph l f}{2c\omega_0^2}\exp\left[\mathrm{i}(kR - \omega t)\right], \tag{19}$$

with the parameter f defined by (9). Both the field E_curl and the magnetic components H_z and H_ρ determined from Eqns (18) contain the resonance factor $\Lambda(\omega)$, the components H_z and H_ρ being phase-shifted by 0.5π relative to E_curl. In the case of grazing incidence of a linearly polarized wave on a dielectric ring, according to these relations, a standing wave forms in the near-field zone of the ring, whose spectrum contains a resonance frequency.

Experiment. In the formulation of experiments, we set ourselves the task of discovering and directly investigating the following main effects predicted by the theory:

(1) discovery of the resonance frequencies at the grazing incidence of a linearly polarized TEM wave on a dielectric ring;

(2) investigation of the effect of the material and object geometry on the main resonance frequencies;

(3) excitation of a resonance magnetic response with a phase change in the reradiated wave and inversion of the resultant magnetic field;

(4) discovery of the resonance interaction of two magnetic dipoles of two dielectric rings.

As is noteworthy, in the fabrication of metamaterials with a negative magnetic response, metallic elements of an extremely small size are used; their characteristics are incorporated into the mathematical model and the integral field of the interaction with the incident wave is found by calculations.

The aim of our investigations was to directly measure the fields near the dielectric ring to obtain the information as accurately as possible and compare it with the results of theoretical calculations. For this, calculations were made of

rings with different geometric dimensions and permittivities in order to select a ring with a size, on the one hand, large enough for measuring the field near it and, on the other, much shorter than the incident wavelength in the resonance frequency domain. Furthermore, the frequency band under study should be accessible and convenient enough for measurements. As a result of several approximations, rings with dimensions of $38 \times 28 \times 5$ mm were made, which had a relative permittivity ~ 200 and a calculated resonance frequency of 1.32 GHz.

The formation of a linearly polarized plane wave in the desired frequency range and the recording of the response of the object under study were effected with an Agilent E5071C ENA series network analyzer with a 300 kHz–20 GHz band, a transmitting horn antenna (3115 Model of ETS Lindgren) for a 0.75–18 GHz frequency band, and a horn antenna (3160-09 Model of ETS Lindgren) for the frequency band 18–26.5 GHz. To improve the signal-to-noise ratio and mitigate the influence of environmental radio noise in the frequency band from 5 MHz to 6 GHz, an additional amplifier with a gain of 20 dB was used. The electric field near the ring was recorded with linear probes with a sensitive element 10 mm in length. The magnetic field was measured with a screened annular probe with a sensitive element 5 mm in diameter. In some experiments, a second horn antenna was used for recording the plane wave behind the ring. To measure the field near the ring and the phase change in the scattered signal, a Tektronix DPO73304DX four-channel pulsed oscilloscope with a bandwidth of 33 GHz was used. To verify the reliability of the data obtained, prior to every measurement, we determined the noise level of the measuring path with connecting cables without the probe in the presence of the incident radiation and the background radiation level with the probe in the presence of the incident radiation without test objects.

To verify the correctness of the diagnostic systems, at the first stage of experiments we studied the known resonance frequencies of the dielectric ring in the arrangement shown in Fig. 1a, when the ring plane was perpendicular to the wave vector and the ring center was on the axis of antenna radiation in the plane of peak emission. Apart from the dielectric ring, a brass ring with the same dimensions was investigated in all experiments.

In the spectral range 12.4–20 GHz, we discovered a resonance frequency of 15.1 GHz, which agrees nicely with the value calculated for this geometry in the framework of the theory of dielectric coaxial resonators [22, 25]. Several oscillation modes can be excited in dielectric rings. This 15.1 GHz frequency is associated with higher azimuthal oscillations excited by the electric component of the incident wave. These oscillations are widely used in various microwave devices. No resonances were found in this range for a brass ring with the same dimensions.

Investigated next were the resonance properties of the dielectric ring arranged according to Fig. 1b, when the ring plane was parallel to the electric vector and perpendicular to the magnetic vector, with the ring center on the axis of antenna radiation. The distance between the antenna and the sensor was 60 cm. The results of the measurements are depicted in Fig. 2. For the dielectric ring, we discovered a resonance frequency of 1.36 GHz, which is excited by the magnetic component of the incident wave. The experimental value of the resonance frequency is slightly different from the theoretical one in (14), which is equal to 1.32 GHz. For the

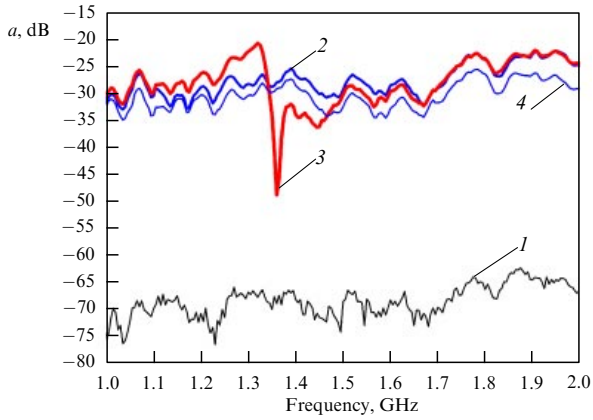

Figure 2. Experimental spectra of the azimuthal vortical electric field outside the ring. Spectra *1*, *2*, and *3* show the noise level, the field level without the ring, and the field at the ring center. Spectrum *3* contains a resonance at a frequency of 1.36 GHz. The spectrum of the metallic ring (curve *4*) is devoid of resonances.

brass ring, no resonances were discovered in this range. Worthy of note is the small width of this resonance, equal to 20 MHz, which is indicative of the low loss in the dielectric ring. This, in turn, provides the possibility of harnessing this effect in the design of new metamaterials with a negative magnetic permeability. We emphasize that so low a loss is unattainable in split-ring metallic resonators [23].

In addition to the role of the material, an important point for the observed resonance is the object shape, even if its volume is kept constant. If we draw an analogy with transmission lines, the geometric shape of the line determines the types of transmitted waves. For the purpose of investigations, the above dielectric ring with a resonance frequency of 1.36 GHz was divided into two equal semirings. The semirings were placed some distance apart and then brought closer so as to form a full ring. Up to virtually a zero separation, when a split ring with a gap of about 0.1 mm was formed, the resonance did not manifest itself (Fig. 3). The resultant resonance is characterized by a shift in the resonance frequency in comparison with that of the initially whole ring. These results can be interpreted using an analogy with the Thomson oscillating circuit.

If the quantity l^{-1} is expressed in terms of the ring self-inductance L in (12) in expression (14) for the frequency ω_0 and the radius r_0 in terms of the cross-sectional ring area $S_0 = \pi r_0^2$, then expression (14) coincides with the classical Thomson formula ($\omega_0^2 = c^2/(LC)$) for the eigenfrequency of an oscillating circuit with the self-inductance L and capacitance $C = \varepsilon S_0/(4\pi d)$, which coincides with the capacitance of a plane capacitor with the plates area S_0 and the gap between the plates equal to the ring circumference $d = 2\pi R$.

By continuing this analogy, we can see how to increase the resonance frequency of the ring dipole without changing either the permittivity ε or the radii R and r_0: it would suffice to divide the ring in halves by two thin radial cuts. By considering the cuts of width s and the halves (with the halves' arc length $\pi R - s$) to be series-connected capacitors with the total capacitance C, we can find the eigenfrequency Ω of this LC circuit by the Thomson formula. For a thin cut ($s \ll \pi R$), we obtain

$$\Omega = \omega_0 \sqrt{1 + \frac{\varepsilon\chi}{2}}, \qquad \chi = \frac{s}{\pi R}, \tag{20}$$

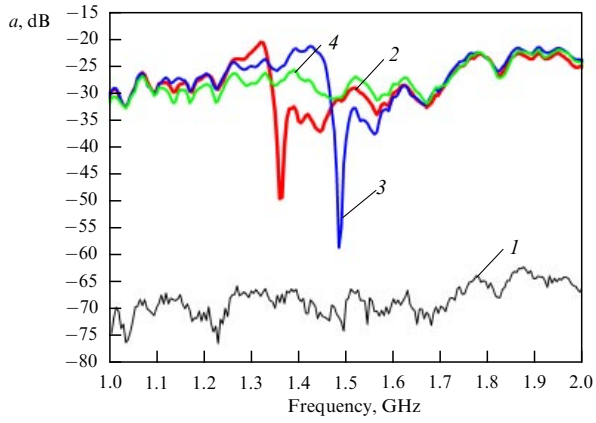

Figure 3. Shift in the resonance frequency of the split-ring magnetic dipole. *1* — noise level, *2* — unsplit-ring spectrum, *3* — spectrum of the ring with a gap 0.01 cm wide, *4* — radiation spectrum without a ring.

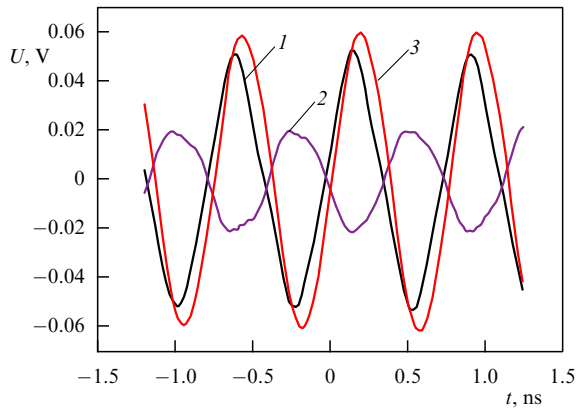

Figure 4. Voltage oscilloscope traces recorded using linear probes of an electric field. Curve *1* — reference probe voltage, curve *2* — voltage of the measuring probe near the distant (from the antenna) side of the dielectric ring, curve *3* — voltage near the dielectric ring side facing the antenna.

where ω_0 is the ring dipole frequency (14). Figure 3 shows the experimentally measured frequency shift caused by the cuts. For an estimate, we assume the values specified in the caption to Fig. 3 to obtain $\Omega/(2\pi) = 1.49$ GHz; therefore, the difference from the measured value is within 1–2%.

5. Alternating-sign magnetic induction of a ring displacement current

As the frequency ω approaches ω_0, the oscillation amplitude of the induced flux Φ_i through a nonconductive ring increases, and in passing to the high-frequency domain $\omega > \omega_0$, the inducing, Φ, and induced, Φ_i, fluxes become oppositely directed [24]. Expressing the relation between Φ and Φ_i as $\Phi_i = \mu\Phi$, we can specify the frequency domain $\omega > \omega_0$ with $\mu < 0$, which corresponds to the inversion of the induction flux and the negative magnetic susceptibility of the ring element. This effect is attended by the indicated reverse direction of the electric and magnetic components of the scattered field, which manifests itself in the change in sign of resonance factor (15) near the resonance frequency.

The phase shift of the resultant resonance oscillations was determined in two ways: using an oscilloscope and two linear electric probes by applying the signal at the resonance frequency of the dielectric ring to an antenna, and using a screened magnetic field probe. In the former case, one probe was used as the reference and was located near the antenna outside the zone of the dielectric ring. The other, measuring, probe was positioned near the ring. The probes were fixed immobile, parallel to vector **E** of the incident wave such that no phase variation of the incident wave occurred between them. In translating the ring relative to the second probe, we directly recorded the signal phase variation relative to the phase of the reference probe signal with the use of a fast-response oscilloscope. The measurement data are depicted in Fig. 4.

It is well known that the effect of resonance scattering of an incident wave involves a phase shift of the scattered wave, which is close to π because of the frequency passage through the resonance value. This effect is attended by a change in the direction of the electric and magnetic components of the scattered field, which shows up in the change in sign of the resonance coefficient $\Lambda(\omega)$ in Eqn (15) near the resonance frequency, thereby providing a resonance lowering of the

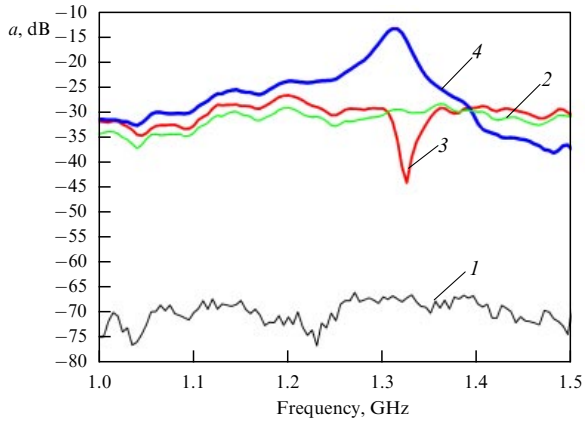

Figure 5. Experimental voltage spectra obtained using a screened annular magnetic field probe. *1* — noise spectrum, *2* — radiation spectrum without the ring, *3* — radiation spectrum outside of the ring, *4* — radiation spectrum inside the ring.

field. In moving the ring relative to the second measuring probe, a phase shift close to π between the ring and reference probe signals was discovered at the dielectric ring side distant from the antenna (curve *2*), which is indicative of the formation of a negative magnetic response of the dielectric ring with a displacement current. It is noteworthy that the amplitude of the signal from the probe located near the front side of the ring facing the antenna (curve *3*) is higher than the amplitude of the signal from the reference probe without the ring (curve *1*) due to the interference of the incident and reflected waves.

In the second case, the change in the magnetic field oscillation phase was recorded with a screened annular magnetic field probe in moving the dielectric ring relative to the probe in the direction of the **k** vector (Fig. 5). The probe diameter was equal to 5 mm, and in measuring the phase shift near the ring surface, the ring was shifted such that the magnetic flux passing through the probe was not screened by the ring surface in the measurements both inside and outside the ring. The resultant data show a resonance enhancement of the magnetic field inside the ring (curve *4* in Fig. 5) and a resonance depression of the magnetic field outside the ring (curve *3* in Fig. 5), which is also indicative

of a phase change between the incident and scattered radiation. The dielectric ring concentrates the magnetic field at resonance. The shift in resonance frequency peaks in these two cases is attributable to the capacitive coupling to the sensor, which lowers the resonance frequency in the case of resonance enhancement of the magnetic field inside the ring.

6. Resonance interaction of magnetic dipoles

The approach developed for a solitary dipole in Sections 4 and 5 can be generalized to a system of dielectric circuits with inductive coupling due to the interference of magnetic fluxes. This interference is characterized by the mutual induction coefficient M of displacement currents in these circuits. Some features of this induction can be understood by considering the magnetic interaction of a pair of similar thin dielectric rings. As is well known [26], the coefficient M depends on the relative position of the rings; in particular, in the simple case of coaxial rings,

$$M = 4\pi R l_2 , \qquad l_2 = \frac{2\wp(q)}{q} ,$$
$$\wp(q) = \left(1 - \frac{q^2}{2}\right) K(q) - E(q) , \tag{21}$$
$$q^2 = \frac{1}{1+\eta^2} , \qquad \eta = \frac{b}{2R} ,$$

where $K(q)$ and $E(q)$ are the complete elliptic integrals of the first and second kinds with the modulus q, and b and R the central distance of the two rings and their radius.

The magnetic fluxes $(\Phi_{\rm i})_{1,2}$ excited by the displacement currents $I_{1,2}$ due to self-induction and mutual induction effects can be represented as

$$(\Phi_{\rm i})_{1,2} = \frac{1}{c}(L I_{1,2} + M I_{2,1}) . \tag{22}$$

We let $\Phi_{01} \exp(-{\rm i}\omega t)$ and $\Phi_{02} \exp(-{\rm i}\omega t)$ denote the respective magnetic fluxes induced by the incidence wave in these rings, and ignore the weak absorption ($\gamma \to 0$) to write the system of equations for the resultant magnetic fluxes Φ_1 and Φ_2 in each of the interacting rings:

$$\frac{1}{\omega_1^2}\frac{\partial^2 \Phi_1}{\partial t^2} + \frac{1}{\omega_2^2}\frac{\partial^2 \Phi_2}{\partial t^2} + \Phi_1 = \Phi_{01} \exp(-{\rm i}\omega t) , \tag{23}$$

$$\frac{1}{\omega_1^2}\frac{\partial^2 \Phi_2}{\partial t^2} + \frac{1}{\omega_2^2}\frac{\partial^2 \Phi_1}{\partial t^2} + \Phi_2 = \Phi_{02} \exp(-{\rm i}\omega t) . \tag{24}$$

The characteristic frequencies of coaxially arranged similar rings, which are defined by the self-inductance of each ring, ω_1, and their mutual inductance, $\omega_{1,2}$, are expressed as

$$\omega_{1,2} = \frac{c\sqrt{2}}{r\sqrt{\varepsilon l_{1,2}}} . \tag{25}$$

Dimensionless quantities l_1 [see (12)] and l_2 [see (21)] describe the self-induction and mutual induction of the rings. The resonance frequencies of coupled oscillations of the pair of coaxial rings are found from system of equations (23), (24):

$$\omega_{\pm} = \frac{\omega_1}{\sqrt{1 \pm l_2/l_1}} . \tag{26}$$

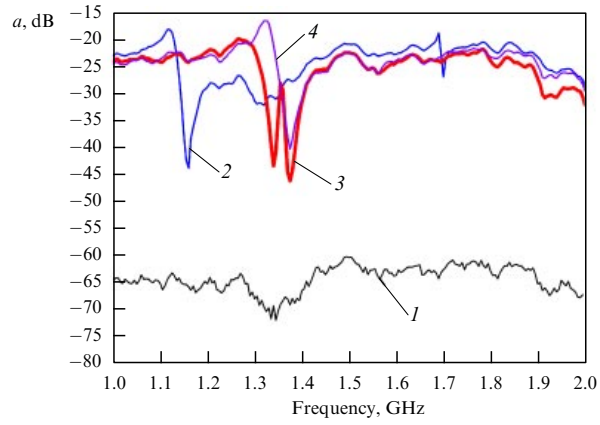

Figure 6. Oscillation spectra of the electric field in the coaxial arrangement of a pair of magnetic resonant ring dipoles. *1* — noise level, *2* and *3* — spectra of the interacting dipoles spaced at 4 and 40 mm, *4* — spectrum of a solitary dipole.

For rings lying in a common plane such that their centers are on the line coinciding with the direction of the incident wave vector **k** (coplanar arrangement), the interaction of magnetic dipoles is also described by system of equations (23), (24). However, in this case, the mutual inductance coefficient M is to be determined by numerical integration or found from experiment. The expression for the resonance frequencies of such a pair of dipoles is a generalization of formula (26):

$$\omega_{\pm} = \frac{\omega_1}{\sqrt{1 \pm M/(4\pi R l_1)}} . \tag{27}$$

When the dipole parameters are known and the resonance frequencies $\omega_{\pm}$ are known, formula (27) allows calculating the mutual inductance coefficient M.

The appearance of two resonance frequencies (26) can be considered a manifestation of the more general effect of the splitting of the spectra of interacting LC circuits [8]. In the special case where the magnetic coupling of the circuits becomes weak ($l_2 \to 0$), the splitting vanishes: $\omega_{\pm} \to \omega_1$.

The experimental oscillation spectra of two magnetic resonance ring dipoles in the form of coaxial dielectric rings are plotted in Fig. 6. The electric field sensor is positioned on the farthest (from the antenna) surface of the lower ring. The upper ring is moved along the symmetry axis. The spectra of the interacting dipoles are clearly seen.

Figure 7 displays the results of measurements for a pair of dielectric rings located in a common plane along the wave vector **k**. The electric field sensor was placed on the farthest (from the antenna) external ring surface. The nearest ring was moved along the **k** vector. As in Fig. 6, the spectra of the interacting dipoles correspond to the oscillatory circuit interaction models under consideration.

7. Dielectric magnetic dipole: a promising element of nanophotonics?

The experiments on the excitation of displacement currents in dielectric ring dipoles outlined in Sections 4–6 illustrate the unusual properties of such dipoles in the case of grazing incidence of exciting electromagnetic waves:

(1) the combination of capacitor and inductor functions in one element;

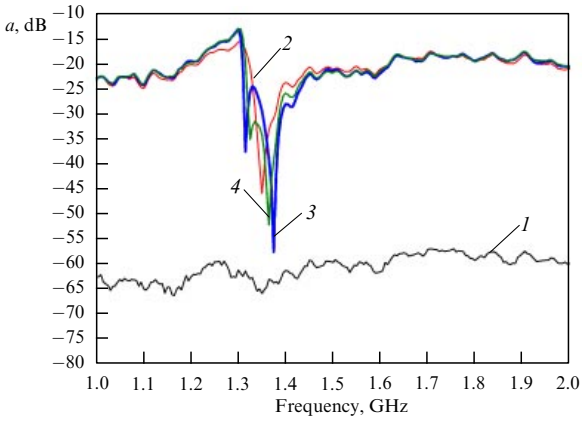

Figure 7. Oscillation spectra of the electric fields induced by a pair of coplanar magnetic resonant ring dipoles aligned with the wave vector **k**. *1* — noise level, *2* — solitary dipole, *3* and *4* — spectra of the interacting dipoles with the ring edges spaced at 10 and 20 mm.

(2) the appearance of a resonance frequency and a narrow resonance line in the dipole excitation spectrum;

(3) a nonuniform magnetic induction field of the dielectric ring;

(4) the formation of negative magnetic susceptibility ($\mu < 0$) of the ring dipole;

(5) the resonance interaction of a pair of magnetic dipoles.

We note that the effect of alternating-sign magnetic susceptibility is shown in Fig. 5 for a GHz range wave in empty space, where the permittivity ε is constant and equal to unity. However, the waveguide propagation of waves makes it possible to investigate the combined action of alternating-sign parameters μ and ε. Specifically, in a nonuniform waveguide containing a tapered section with a critical frequency ω_c, the wave field with a frequency $\omega < \omega_c$ decays exponentially in the tapered section. For low-frequency waves, $\omega < \omega_c$, this section simulates a medium with an effective negative permittivity $\varepsilon_{\text{eff}} < 0$ [27]. If this element contains elements with $\mu < 0$, this structure corresponds to a metameterial with a negative refractive index [28]

$$n_1 = -\sqrt{\left(-|\varepsilon_{\text{eff}}|\right)\left(-|\mu|\right)} < 0\,. \tag{28}$$

The transmission spectrum of GHz radio waves tunneling in the waveguide through an aperture of a metamaterial as in (28) was measured in Ref. [29]. In this case, values $\mu < 0$ were produced by Pendry's split metallic resonators consisting of two concentric open metallic rings [23] (with inevitable ohmic loss). By contrast, a system of dielectric magnetic dipoles located in the waveguide permits simulating low-absorption metamaterials using a microwave transmission line.

It is significant that the theoretical concept of dielectric magnetic dipoles reliant on Faraday's magnetic induction (see Section 3) [30] is not limited, as with metallic resonance elements, to radio frequencies and can be extended to higher frequencies, in particular to the IR range, and ultimately to the visible range of the spectrum. In this case, the passage from the GHz range to the optical one should be attended by a decrease in sizes of the subwavelength transmitting and receiving devices. However, optical elements whose size is comparable to the wavelength of light cannot be produced by scaling down radio engineering devices. Such nanodimensional elements require new physical principles and a new technology: specifically, the subwavelength oscillating circuit described in [15] consists of a glass ball 20 nm in radius (capacitor) coated with a thin silver shell (inductor). A resonator for IR waves in the form of a 20 nm thick metallic horseshoe 300–400 nm in size, deposited on a quartz substrate, was developed in [31]. These elements make up three-dimensional periodic structures with periods of several hundred nanometers; the Q factor of such elements is limited by the ohmic loss in their metallic parts.

The development of new low-loss all-dielectric oscillatory circuits of the optical range has aroused growing interest in the electrodynamics of displacement currents [32]. The use of metamaterials has opened a new path for introducing nanooptical structures into electronics. Optical analogues of GHz dielectric resonance magnetic dipoles, which combine the properties of a nanocapacitor and nanoinductor in one element, appear to be promising elements of such structures. The main geometric parameter determining the eigenfrequency ω_0 of this nanodimensional ring dipole is, according to formula (14), its short radius r_0. For instance, setting $r_0 = 40$ nm and $R = 400$ nm for a dielectric ring with $\varepsilon \approx 5$, we obtain $\omega_0 = 2.9 \times 10^{15}\ \text{s}^{-1}$, which corresponds to a visible-range wavelength $\lambda \approx 650$ nm in empty space. A three-dimensional periodic lattice of magnetic dipoles can be regarded as a model of a dielectric metacrystal with alternating-sign magnetic response in the optical and infrared ranges.

Direct experimental investigations of separate units of the nanodimensional lattice are difficult to perform. But these investigations are central to the optimization of the physical and geometrical parameters of large nanocell arrays. This optimization is of interest from the standpoint of the development of artificial optoelectronic materials, in particular, for optical magnetic dipole radiators [33], dielectric antennas [34], and nanosystems characterized by the simultaneous excitation of electric and magnetic resonance modes [35]. The electromagnetic properties of these optical structures can be conveniently simulated using radio frequency oscillatory systems containing solitary resonant dipoles of the GHz range [36].

The advent of nanoelectronics has made it possible to employ the notion of displacement currents in so rapidly developing an area as applied optics. This development has drawn attention to new, so far purely academic, problems; one of them follows directly from formula (1), which relates the displacement current to the fast change in the electric induction $\mathbf{D} = \varepsilon\mathbf{E}$ in the medium. Still being discussed is the generation of displacement currents caused by variations in the electric field $\mathbf{E}$ for a stationary value of the permittivity ε. Another mechanism of generating this current is also possible, via the transient permittivity described by the derivative $\partial\varepsilon/\partial t$ in the displacement current definition, Eqn (1). In particular, discussed in the literature is the mechanism of eigenmode generation in a resonator filled with a dielectric with a time-dependent ε. This dependence can be caused, for instance, by fast permittivity modulation induced by a laser pump, which results in a resonator spectrum transformation [37]. Attention is also drawn to suggestions to use rapid ε variations to imitate relativistic effects predicted by quantum electrodynamics: the transformation of quantum fluctuations of the vacuum to observable photons [38] and the dynamic Casimir effect [39]. However, these problems are still to be solved.

Acknowledgements
The authors express their appreciation to O F Petrov and A G Khrapak for their support of the work and the fruitful discussions.

References

1. Shvartsburg A B, Maradudin A A *Waves in Gradient Metamaterials* (New Jersey: World Scientific, 2013)
2. Silveirinha M, Engheta N *Phys. Rev. Lett.* **97** 157403 (2006)
3. Zhao Q et al. *Appl. Phys. Lett.* **92** 051106 (2008)
4. Chervyakov G G, Razdobud'ko V V *Vvedenie v Radiooptiku* (Introduction to Radiooptics) (Moscow: Uchebnaya Literatura, 2009)
5. Engheta N *Science* **317** 1698 (2007)
6. Miroshnichenko A E et al. *Opt. Photon. News* **23** 35 (2012)
7. Busch K et al. *Phys. Rep.* **444** 101 (2007)
8. Landau L D, Lifshitz E M *Electrodynamics of Continuous Media* (Oxford: Pergamon Press, 1984); Translated from Russian: *Elektrodinamika Sploshnykh Sred* (Moscow: Nauka, 1992)
9. Liu R et al. *Phys. Rev. Lett.* **100** 023903 (2008)
10. Rand S C, Fisher W M, Oliveira S L *J. Opt. Soc. Am. B* **25** 1106 (2008)
11. Wang J et al. *J. Appl. Phys.* **109** 084918 (2011)
12. Evlyukhin A B et al. *Nano Lett.* **12** 3749 (2012)
13. O'Brien S, Pendry J B *J. Phys. Condens. Matter* **14** 4035 (2002)
14. Kapitanova P et al. *Sci. Rep.* **7** 731 (2017)
15. Semouchkina E et al. *Appl. Phys. Lett.* **96** 233503 (2010)
16. Wu Z S, Wang Y P *Radio Sci.* **26** 1393 (1991)
17. Evlyukhin A B et al. *Phys. Rev. B* **82** 045404 (2010)
18. Smith D D, Fuller K A *J. Opt. Soc. Am. B* **19** 2449 (2002)
19. Geffrin I M et al. *Nature Commun.* **3** 1171 (2012)
20. Staude I et al. *ACS Nano* **7** 7824 (2013)
21. Maslov A V et al. *J. Opt.* **16** 125104 (2014)
22. Il'chenko M E (Ed.) *Dielektricheskie Rezonatory* (Dielectric Resonators) (Moscow: Radio i Svyaz', 1989)
23. Pendry J B et al. *IEEE Trans. Microwave Theory Tech.* **47** 2075 (1999)
24. Sigov A S, Shvartsburg A B *Dokl. Phys.* **61** 313 (2016); *Dokl. Ross. Akad. Nauk* **469** 38 (2016)
25. Pozar D M *Microwave Engineering* (Hoboken, NJ: Wiley, 2012)
26. Alù A, Salandrino A, Engheta N *Opt. Express* **14** 1557 (2006)
27. Ranfagni A et al. *Phys. Rev. E* **63** 025102(R) (2001)
28. Veselago V G *Sov. Phys. Usp.* **10** 509 (1968); *Usp. Fiz. Nauk* **92** 517 (1967)
29. Baena J D et al. *Phys. Rev. B* **72** 075116 (2005)
30. Lagarkov A N et al. *Phys. Usp.* **52** 959 (2009); *Usp. Fiz. Nauk* **179** 1018 (2009)
31. Grigorenko A N et al. *Nature* **438** 335 (2005)
32. Jahani S, Jacob Z *Nature Nanotechnol.* **11** 23 (2016)
33. Schmidt M K et al. *Opt. Express* **20** 13636 (2012)
34. Filonov D S et al. *Appl. Phys. Lett.* **100** 201113 (2012)
35. Fu Y H et al. *Nature Commun.* **4** 1527 (2013)
36. Shvartsburg A B et al. *Sci. Rep.* **7** 2180 (2017)
37. Kawakubo T, Yamamoto K *Phys. Rev. A* **83** 013819 (2011)
38. Walther H et al. *Rep. Prog. Phys.* **69** 1325 (2006)
39. Wilson C M et al. *Phys. Rev. Lett.* **105** 233907 (2010)